

Obtaining carbon structures from organic compounds derived of biomass for their use in chemical sensors manufacturing

M.-R. MARINESCU^{a,b}, E. DAVID^c

^aNational Institute for Research and Development in Microtechnologies –IMT Bucharest, Erou Iancu Nicolae 126A, 077190 Voluntari, Ilfov, Romania

^bUniversity Politehnica of Bucharest, 313 Splaiul Independentei, Sector 6, 060042, Bucharest, Romania

^cNational Research Institute for Cryogenic & Isotopic Technologies, ICSI Rm. Valcea Uzinei No.4; P.O. Raureni, P.O. Box 7; 240050 Rm. Valcea, Romania

In this paper, organic compounds derived from biomass (ethanol, toluene, phenol, 1-methylnaphthalene) were catalytically decomposed and reformed with steam over Fe/Al₂O₃ for obtaining of carbon nanotubes (CNTs), materials used in chemical sensors manufacturing for applications in medical devices or in optoelectronics. In the decomposition reaction, the oxygen functional group in ethanol and phenol initiated the hydrogen and CNTs production, while a low amount of toluene and 1-methylnaphthalene were cracked, resulting hydrogen and amorphous carbon. In the reforming reaction, the hydrogen and CNTs yields sharply increased, more than 80% of ethanol and toluene was converted to CNTs. From 1-methylnaphthalene low amounts of CNTs were obtained.

(Received February 27, 2020; accepted April 9, 2020)

Keywords: Biomass derived organics, Decomposition reaction, Steam reforming, Fe/Al₂O₃ catalyst, Carbon structures (CNTs)

1. Introduction

Although the carbon can exist in different forms of polymeric structures, only the quasi-crystalline forms have found a significant use in medical devices [1-3]. The carbon materials are intensively studied due to their great mechanical, electrical, thermal, and optical properties [4]. These carbon structures are based on the hexagonal crystal structure of graphite [1, 2]. In graphite, the atoms of carbon are linked by covalent bonds into planar (hexagonal arrays). The carbon-carbon bond energy within the carbon layers is very high (114 kcal/mole), the binding between the layers is of the relatively weak van der Waals type, with a bond energy of about 4 kcal/mole [3, 5-7]. As a consequence of the anisotropic bonding, many of the graphite crystal properties are highly anisotropic. In addition to the variations in properties that can occur because of anisotropy of the perfect graphite crystals, the properties of imperfect graphite crystals depend on the concentration and type of crystalline defects [8-10]. In such crystals, the imperfections, most times lead to extraneous linkages between layers which could be used as an advantage in obtaining of carbon materials with high mechanical properties [8, 11]. The structure of the strongest carbon materials is far from perfect, but the structure can be improved, by different techniques and using various raw materials [11-14]. Carbon nanotubes (CNTs), as new carbon structures, have special physical and chemical characteristics and have numerous potential applications such as in the areas of biosensors, carbon

electronics, catalysis, hydrogen storage, etc [2, 13]. CNTs have great potential in increasing the power factor of devices. They can convert thermal energy into electric energy [15]. In the last years, the production of CNTs has significantly increased to meet the needs of such applications. The hydrocarbons (for example methane, ethylene, acetylene, benzene, etc) were widely used to obtain CNTs by the technique of catalytic chemical vapor deposition (CCVD) [2, 12].

Bio-tar resulting as a by-product during thermal biomass conversion, depends on different processes used (up to 70 wt% for pyrolysis process [14, 17] and up to 20 wt% for gasification process [14]) and is a mixture of organic compounds, mainly of alcohols, phenols, one-ring aromatic hydrocarbons (benzene, toluene, etc), two-ring aromatic hydrocarbons (naphthalene and 1-methylnaphthalene, etc) [6, 7]. In addition, the bio-tar composition derived from biomass pyrolysis process such as its high water content, the instability of chemical properties are suitable for steam reforming process to obtain carbon structures and hydrogen [8, 9, 18, 19]. The biomass derived organics, such as bio-ethanol and bio-tar, contains different types of organic compounds, however, the effect of these organic compounds on production of carbon structures and hydrogen too little has been investigated.

In this study, ethanol, toluene, phenol and 1-methylnaphthalene, have used as organic components derived from biomass, representing C₂ and phenolic compound with oxygen functional group, and one-ring, two-ring aromatic hydrocarbons. These organic

compounds were decomposed using a catalyst (without steam) and also reformed (with steam) over Fe/Al₂O₃ catalyst, using a fixed bed reactor. To characterize the catalyst and the resulted carbon structures, a series of analysis methods, such as scanning electron microscopy (SEM), temperature programmed oxidation coupled with mass spectrum (TPO-MS) and transmission electron microscopy (TEM) were used. The influences of organic compounds type (C2, one aromatic ring and two aromatic rings hydrocarbons), on production of hydrogen and CNTs structures were investigated. They can show great potential for use in chemical sensors manufacturing and in optoelectronics applications.

2. Experimental part

Alumina (Al₂O₃), grain size of 40 to 20 mesh, as support material was purchased from Sigma-Aldrich Company. The Al₂O₃ was calcined at 1050°C for 3 hours. The Fe/Al₂O₃ catalyst with 10% Fe loading was obtained by impregnation method in a rotary evaporator at 70°C using an aqueous solution of FeSO₄·7H₂O (Sigma-Aldrich Company). After impregnation, the sample was dried at 110°C for 12 h and then calcined at 600°C for 6 h under air atmosphere.

The catalytic decomposition/reforming reaction of ethanol, toluene, phenol and 1-methylnaphthalene were performed in a fixed bed quartz reactor (i.d. 5 mm) under atmospheric pressure. Before the reactions, 1 ± 0.05 g of catalyst was reduced in a 80 mL/min of 30% H₂/Ar gas flow at 600°C for 2 h. Then, the reactor was stripped with Ar (99.999 vol% purity), and the reaction temperature was held at 600°C. In the reforming reaction, one of the organic compounds (including ethanol, toluene, phenol and 1-methylnaphthalene) and distilled water were fed into a preheater by injection. Then they were evaporated at 315°C and carried by 80 mL/min Ar to the Fe/Al₂O₃ catalyst bed.

Since the phenol is in solid form at room temperature, a solution of 8 wt% phenol in water was used for phenol injection. In the decomposition reaction, experimental conditions were the same as for the reforming reaction. The majority of gas was passed through the condensing system to remove the unreacted organic compounds and water. The gas fraction was collected and analyzed by a GC analyzer (3000A, Agilent). After 1 hour experiment, the resulted liquid fraction and Fe/Al₂O₃ spent catalyst were collected. The TPO-MS experiments (temperature-programmed oxidation coupled with mass spectrum) of Fe/Al₂O₃ spent catalyst and graphite were performed to determine the content of solid carbon. The analytical system, capable of performing TPO with seamless data acquisition from the in-bed thermocouple used was Hiden Analytical CATLAB-PCS

Based on the quantification of carbon amount in the gas/liquid/solid fraction, carbon balance could be calculated. To evaluate the performance of Fe/Al₂O₃ catalyst, the carbon conversion and carbon balance were estimated using the following formulas:

$$C_{conversion} (\%) = \frac{m(CO) + m(CO_2) + m(CH_4) + m(solid)}{m(organic\ compound)} \times 100 \quad (1)$$

$$C_{balance} (\%) = \frac{m(CO) + m(CO_2) + m(CH_4) + m(liquid) + m(solid)}{m(organic\ compound)} \times 100 \quad (2)$$

where m represents the total molar of carbon in each component.

The scanning electron micrograph (SEM) images of the catalysts and solid products were measured using a FEI Quanta 400 SEM analyzer, equipped with X-ray energy dispersive spectrometer (EDS). The transmission electron microscope (TEM) images of CNTs structures were recorded using JEOL JEM-3010 high-resolution transmission electron microscope (HRTEM). X-ray diffraction (XRD, Cu K α , 50 kV, 300 mA, in air at room temperature) was used to characterize the catalyst.

3. Results and discussions

3.1. Catalyst characterization

Fig. 1 presents the XRD pattern of the reduced Fe(10wt.)/Al₂O₃ catalyst and only the peaks for Fe metal and Al₂O₃ can be seen in the XRD diagram, this indicating that the Fe/Al₂O₃ catalyst has been reduced at 600°C.

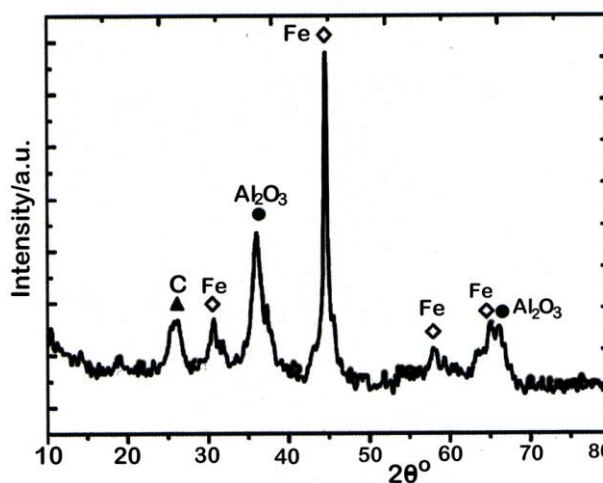
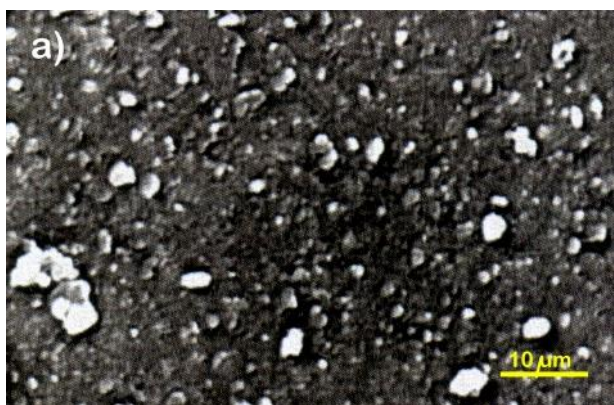
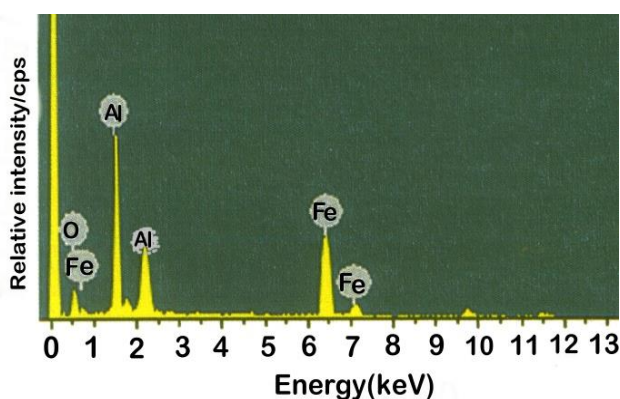


Fig. 1. XRD pattern of the reduced Fe(30 mol%)/Al₂O₃ catalyst at 600°C

Fig. 2 (a) shows the SEM image for the surface morphology of Fe(10 wt.)/Al₂O₃ catalyst after hydrogen reduction at 600°C.



(a)



(b)

Fig. 2. (a) SEM image for the surface morphology of Fe(10 wt.)/Al₂O₃ catalyst after reduction with hydrogen at 600 °C and (b) EDS pattern of the Fe(10 wt.)/Al₂O₃ catalyst

It can be observed that the Fe metallic particles were formed uniformly on the Al₂O₃ support and only a few particles were aggregated together. EDS analysis of the Fe(10wt.)/Al₂O₃ catalyst presented in Fig. 2b shows the presence of Fe, Al and O elements that is consistent with the XRD results.

3.2. The yield of carbon deposition

In the decomposition and reforming reactions, the solid carbon particles resulted from the decomposition of organic compounds were deposited on the surface of Fe/Al₂O₃ catalyst. The quantity of deposited carbon from organic compounds is presented in Fig. 3. The highest amount of carbon resulted from the decomposition of ethanol.

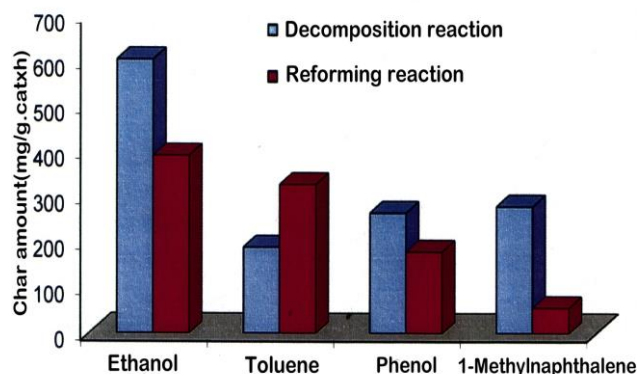


Fig. 3. Carbon amounts that resulted from organic compounds in the decomposition and reforming reactions

Due to the high degree of conversion of carbon from ethanol, more intermediate products were resulted and these were decomposed to carbon on the surface of Fe/Al₂O₃ catalyst. The lowest carbon deposition was obtained from toluene and it was attributed to the low carbon conversion in the decomposition reaction. In this reaction, the amount of deposited carbon increased in the next order: toluene < phenol < 1-methylnaphthalene < ethanol. On the other hand, in the reforming reaction, the amount of deposited carbon decreased in the order of ethanol > toluene > phenol > 1-methylnaphthalene, in accordance with the order of carbon conversion for these organic compounds. The carbon amount increased from 190 to 328 mg/(g-cata*h) for toluene after the addition of steam and this may be attributed to the steam effect on the formation of carbon deposit.

Compared with that in decomposition reaction, the carbon conversion of toluene sharply increased to 328 mg/(g-cata*h), and the more carbon species increased the formation of carbon deposition in the reforming reaction.

3.3. Types of deposited carbon structures

The proportions of different types of deposited char are showed in Fig. 4. As can be seen, in the decomposition reaction of toluene, phenol and 1-methylnaphthalene (Fig. 4 a, b), the nascent carbon and amorphous carbon were the main types of deposited carbon structures, and the amount of CNTs was under 20 wt.%.

The highest amount of amorphous carbon was around of 70wt% and resulted after the decomposition reaction of 1-methylnaphthalene. This means that in decomposition reaction of the organics of high molecular weight and without oxygen functional group (such as 1-methylnaphthalene) has mainly formed of amorphous carbon.

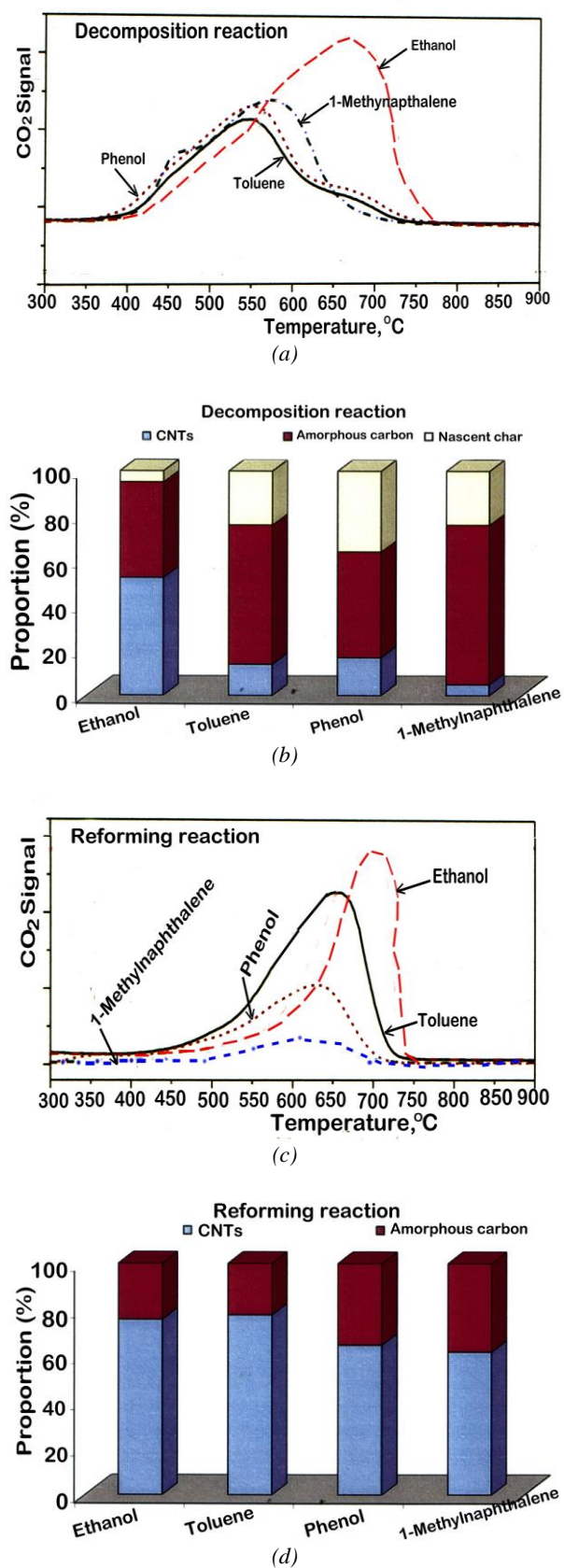


Fig. 4. TPO-MS analysis of carbon materials: (a), (b) for decomposition reaction; (c), (d) for reforming reaction, and the proportions of different types of deposited carbon structures

On the other hand, in the decomposition reaction of ethanol, the carbon nanotubes were the main type of deposited carbon structure. In the reforming reaction, the nascent carbon was reformed by steam, the steam addition significantly increased the amount of CNTs and the formation of amorphous carbons was reduced.

The amount of CNTs were around 60% after the phenol and 1-methylnaphthalene reforming, and over 70% for toluene and ethanol reforming. The growth of CNTs structures needed to complete with the formation of amorphous carbon during the decomposition or reforming reaction, the consumption of amorphous carbon causing the growth of CNTs structure. Comparing these tested organic compounds (ethanol, toluene, phenol and 1-methylnaphthalene), the CNTs amount that resulted from toluene and ethanol was bigger than those from phenol and 1-methylnaphthalene after the reforming reaction (Fig. 4 c,d).

Fig. 5 shows the SEM images of carbon structures that were deposited on Fe/Al₂O₃ catalyst surface during the decomposition and reforming reactions. A carbon nanotubes structure with several micrometers length was detected on the surface of catalyst after the ethanol and phenol decomposition.

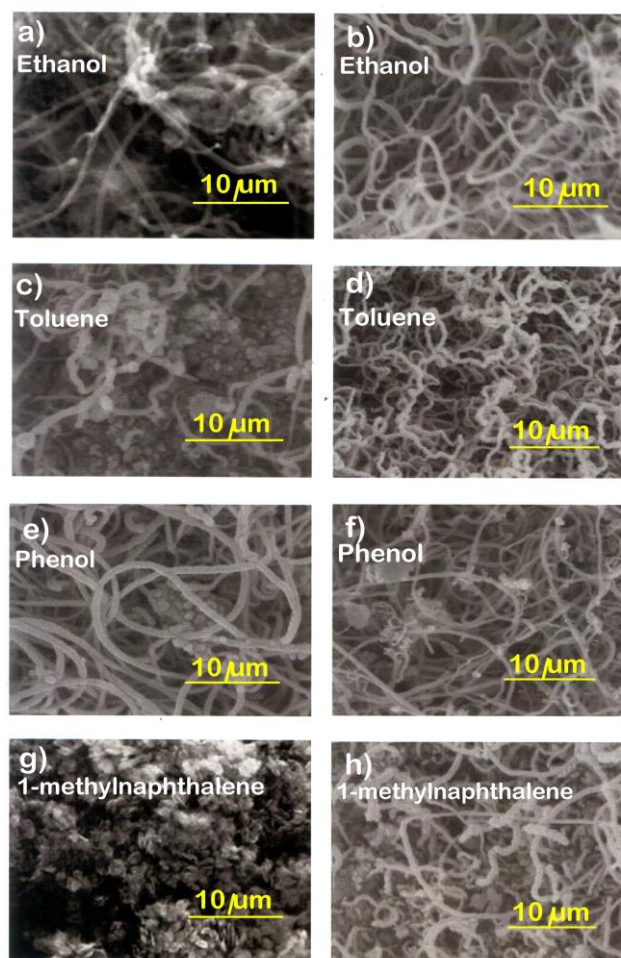


Fig. 5. SEM images of carbon materials (a, c, e, g- in decomposition reaction; b, d, f, h- in reforming reaction)

As respects the decomposition reaction of toluene and 1-methylnaphthalene, CNTs structure was very rarely produced, and only a few particles of amorphous carbon detected on the catalyst surface. In the reforming reaction, the amount of CNTs quickly increased, CNTs structures being observed on the catalyst surface after the reforming reaction of ethanol and toluene. With respect to the decomposition of 1-methylnaphthalene, the amorphous carbon structure was observed to be the main type of deposited carbon, which covered the active sites on the catalyst surface and lead to catalyst deactivation. A high carbon conversion could supply much more carbon species and these will promote the CNTs growth, this means that the carbon species for the growth of CNTs are mainly formed in the cracking reaction of organic compounds, rather than in the polymerization reaction of aromatic rings. The organic compounds with low molecular weight and low unsaturation degree (in this case the ethanol) were easily cracked to different carbon species and they promoted the CNTs formation, while the organic compounds of high molecular weight and high unsaturation degree (such as 1-methylnaphthalene) favored the deposition of amorphous carbon. Fig. 6 shows the TEM images of spent catalysts. The support material, Fe particles and CNTs were observed.

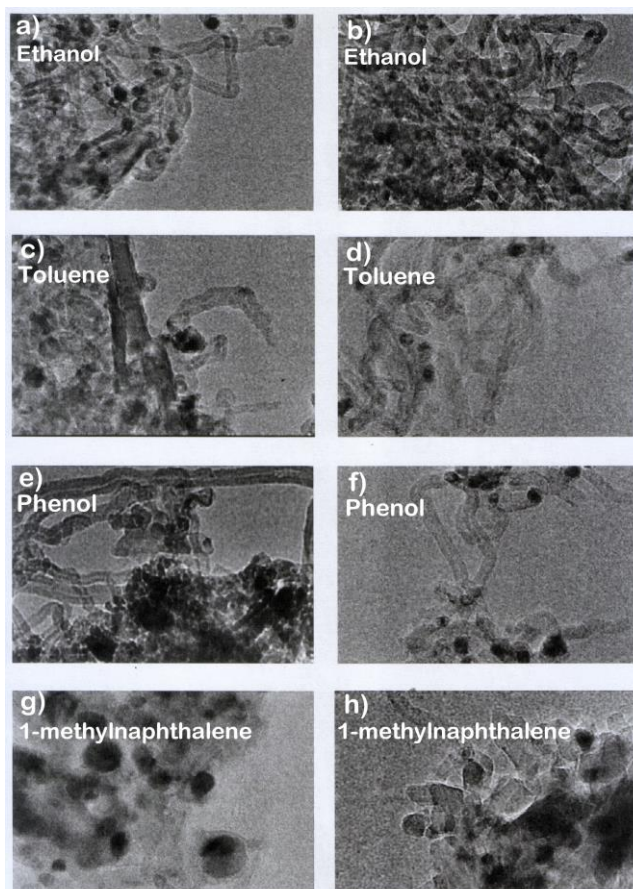


Fig. 6. TEM images of spent catalysts (a, c, e, g- after decomposition reaction; b, d, f, h,- after reforming reaction)

The Fe particles were also observed together with CNTs after the decomposition and reforming reactions of organic compounds. From the analysis of TEM images, the presence of Fe particles and CNTs it is obvious. The CNTs were mainly formed on the small Fe particles during the decomposition of ethanol and the reforming of aromatic compounds. Besides the particle size of Fe catalyst, the quantity of CNTs was also influenced by the nature of organic compounds and steam addition in the reforming reaction.

4. Conclusions

Biomass-derived organic compounds (such as ethanol, toluene, phenol and 1-methylnaphthalene) were subject to catalytic decomposition and reforming reactions for the production of carbon structures (amorphous carbon and nanotubes). After decomposition reaction of the organic compounds with functional group containing oxygen (ethanol and phenol) resulted hydrogen and CNTs, while a small quantity of H₂ and amorphous carbon were obtained from toluene and 1-methylnaphthalene. On the other hand, the organic compound of high molecular weight and without functional group containing oxygen favored the amorphous carbon formation. In the reforming reaction, the yield of CNTs significantly increased and the reforming by steam of amorphous carbon determined the CNTs growth. Besides Fe catalyst particle size, the type of organic compound and steam addition in reaction have influenced the quantity of CNTs. Because of their outstanding mechanical stability and electric transport properties, CNTs have become one of the most popular pure carbon materials and suitable to be use in chemical sensors manufacturing for applications in different sectors, such as medical devices, industry, environment protection, energy. For this reason, the development of new methods of CNTs obtaining by using new sources of raw materials (such as biomass-derived organic compounds) represents a challenge and a necessity.

Acknowledgments

This work was supported by the European Social Fund from the Sectoral Operational Programme Human Capital 2014-2020, through the Financial Agreement with the title "Scholarships for entrepreneurial education among doctoral students and postdoctoral researchers (Be Antreprenor!)", Contract no. 51680/09.07.2019 – SMIS code: 124539.

References

- [1] R. H. Baughman, A. A. Zakhidov, W. A. de Heer, *Science* **297**(5582), 787 (2002).
- [2] J. Ashok, S. Kawi, *Int. J. Hydrogen Energy* **38**(32), 13938 (2013).
- [3] K. A. Shah, B. A. Tali, *Mater. Sci. Semicond. Process*

- 41**, 67 (2016).
- [4] A. V. Kukhta, S. A. Maksimenko, M. I. Taoubi, M. Harb, A. Cataldo, S. Bellucci, V. I. Nuzhdin, V. F. Valeev, A. L. Stepanov, *Optoelectron. Adv. Mat.* **13**(5-6), 354 (2019).
- [5] D. Li, M. Tamura, Y. Nakagawa, K. Tomishige, *Bioresour. Technol.* **178**, 53 (2015).
- [6] F. M. Josuinkas, C. P. B. Quitete, N. F. P. Ribeiro, M. M. V. M. Souza, *Fuel Process Technol.* **121**, 76 (2014).
- [7] H. Dai, *Acc. Chem. Res.* **35**, 1035 (2002).
- [8] G. L. Agafonov, I. Naydenova, P. Vlasov, J. Warnatz, *Proc. Combust. Inst.* **31**(1), 575 (2007).
- [9] A. L. Alberton, M. M. V. M. Souza, M. Schmal, *Catal Today* **123**(1), 257 (2007).
- [10] W. Joseph, *Electroanalysis* **17**, 7 (2005).
- [11] A. Bianco, K. Kostarelos, C. D. Partidos, M. Prato, *Chem. Commun.*, 41 (**5**), 571 (2005).
- [12] K. Hernadi, A. Fonseca, J. B. Nagy, A. Siska, I. Kiricsi, *Appl. Catal. A Gen.* **199**(2000), 245 (1999).
- [13] K. A. Shah, B. A. Tali, *Mater. Sci. Semicond. Process* **41**, 67 (2016).
- [14] C. Li, K. Suzuki, *Resour. Conserv. Recycl.* **54**(11), 905 (2010).
- [15] N. Fatima, Kh. S. Karimov, J.-U. Nabi, H. Meng, Z. Ahmad, M. Riaz, M. Mehran Bashir, M. I. Khan, R. Ali, A. Khan, F. Touati, *J. Optoelectron. Adv. M.* **21**(5-6), 333 (2019).
- [16] T. Furusawa, K. Saito, Y. Kori, Y. Miura, M. Sato, N. Suzuki, *Fuel* **103**, 111 (2013).
- [17] S. Xiu, A. Shahbazi, *Renew Sustain Energy Rev.* **16**(7), 4406 (2012).
- [18] S. Wang, Q. Cai, J. Chen, L. Zhang, L. Zhu, Z. Luo, *Fuel* **160**, 534 (2015).
- [19] A. B. Dongil, L. Pastor-Perez, N. Escalona, A. Sepulveda-Escribano, *Carbon* **101**, 296 (2016).

*Corresponding author: roxana.marinescu@imt.ro